JZUS

Automatic inspection of LED indicators on automobile meters based on a seeded region growing algorithm

Hong ZHOU[†], Hai-er XU[†‡], Pei-qi HE, Zhi-bai SONG, Chen-ge GENG

(*Department of Instrument Science and Engineering, Zhejiang University, Hangzhou 310027, China*)

[†]E-mail: zhouh@mail.bme.zju.edu.cn; haierxu0109@gmail.com

Abstract: Light emitting diode (LED) indicators used on automobile meters are essential for safe driving and few errors can be tolerated. The current manual inspection approach can achieve only 95% accuracy rate in weeding out errors occurring in the production process. It is imperative to improve the accuracy of the inspection process to better achieve the goal of safe driving. This paper proposes an automatic inspection method for LED indicators for use on automobile meters. Firstly, red-green-blue (RGB) color images of LED indicators are acquired and converted into R, G, and B intensity images. A seeded region growing (SRG) algorithm, which selects seeds automatically based on Otsu's method, is then used to extract the LED indicator regions. Finally, a region matching process based on the seed and three area parameters of each region is applied to inspect the LED indicators one by one to locate any errors. Experiments on standard automobile meters showed that the inspection accuracy rate of this method was up to 99.52% and the inspection speed was faster compared with the manual method. Thus, the new method shows good prospects for practical application.

Key words: Automatic inspection, Light emitting diode (LED) indicators, Automobile meter, Seeded region growing (SRG)
doi:10.1631/jzus.C0910144   **Document code:** A   **CLC number:** TP2; TP391.41
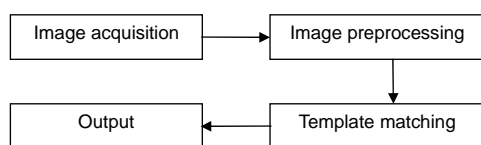
1 Introduction

New technologies are applied to automobile manufacture with each passing day. To support a safer driving environment for drivers, the number of LED indicators used on automobile meters is also increasing rapidly. For example, the Yutong Bus (Zhengzhou Yutong Co., Ltd., China) has a total of up to 45 surface mount technology (SMT) LED indicators on the meter, accounting for almost a quarter of its total cost of production. With these LED indicators, the automobile meter can keep drivers better informed as they provide a lot of immediate information relevant to the automobile. In general, LED indicators can be divided into three groups: (1) blue or green LED indicators which are used to display the status of automobile applications such as turning signals, headlights or fog lights; (2) yellow LED indicators

which are used to alert drivers to failures of systems such as the anti-lock braking system (ABS) or engine self-check; (3) red LED indicators which are used to warn the drivers of unsafe driving conditions such as engine cooling water temperatures or oil pressures that are too high for continued operation. Faulty LED indicators on automobile meters are unsafe for drivers and the consequences of failure to warn drivers could be catastrophic. However, in the Chinese automobile industry, because of missing components, LED damage or improper manual welding (which frequently happens during the meter production process), errors such as malfunctions, lack of brightness leading to poor recognition, or incorrect color often occur in these LED indicators. To locate these errors, inspection of the LED indicators is necessary during the automobile meter testing process. Currently, the traditional manual inspection approach is widely used in which the indicators are checked mechanically one by one with a low efficiency. Moreover, with the ever growing number of indicators, manual errors

(erroneous inspection or inspections that fail to detect faults) caused by visual fatigue cannot be avoided and the successful inspection rate is only 95%. Therefore, developing an automatic inspection method for LED indicators to replace manual inspection as a way of improving production quality and efficiency is essential to the mass production of automobile meters.

So far, few automatic inspection methods for LED indicators used in automobile meters have been developed. However, many methods have been developed from related research on the inspection of industrial products using machine vision, such as automatic printed circuit board (PCB) inspection (Moganti *et al.*, 1996), integrated circuits (IC) wafer inspection (Wu *et al.*, 2008), surface roughness inspection (Lee and Tarng, 2001), cathode ray tube (CRT) panel auto-inspection (Perng *et al.*, 2007), fabric detection (Ghazi Saeidi *et al.*, 2005; Kumar, 2008), and LED wafer inspection (Chang *et al.*, 2009). The industrial visual system (IVS) (Newman and Jain, 1995; Malamas *et al.*, 2003) is an industrial inspection method based on machine vision. The image of an inspected product is first acquired using visual devices, and this image is then compared with a template so as to evaluate the quality of the inspected product. Fig. 1 illustrates the general processes of the IVS model. After image acquisition, image preprocessing plays a key role in extracting the characteristic features of objects to implement the template matching process.

Fig. 1 General processes of the industrial visual system (IVS) model

In this paper, an automatic inspection method based on the IVS model is proposed for locating faults in LED indicators made for use in automobile meters. To extract the characteristic features of LED indicator regions, LED indicator images need to be segmented. There are four main approaches to image segmentation (Pal and Pal, 1993; Zhang, 1996; Adamek *et al.*, 2005): threshold methods, boundary-based methods, region-based methods, and hybrid methods. The seeded region growing (SRG) algorithm (Adams and

Bischof, 1994; Wu *et al.*, 1996; Ikonomatakis *et al.*, 1997; Tuduki *et al.*, 2000) is the method typical of region-based segmentation. Compared with simple threshold techniques, SRG is more time-consuming, but it retains more information at the boundaries of the region, which can enhance the effectiveness of the extraction for the LED indicator regions. Compared with boundary-based methods or hybrid methods, SRG is a more rapid, robust, and easy-to-use approach to image segmentation (Adams and Bischof, 1994). It performs a segmentation of an image with respect to a set of points known as seeds, and groups neighboring pixels or a collection of pixels with similar properties into larger regions. In the SRG algorithm, the seeds can be selected automatically based on Otsu's method (Otsu, 1979; Buxton *et al.*, 2007). SRG is applied to select the seeds automatically and to extract the LED indicator regions in LED indicator images. If the LED indicators are not functioning properly or the brightness is too low for them to be seen with the naked eye, no proper points can be selected as seeds from the corresponding regions. Thus, the seeds can be used to judge whether the functionality or the brightness is up to standard. As the region areas differ in color (in general, LED indicators have one of four colors: red, green, blue or yellow), they can also be used to judge whether the color is correct. Thus, the seed and region area of each LED indicator region are considered as the characteristic features to match to a set template. If there is no match, the indicator errors would be detected. The main processes of this method will be described in the following algorithm model section.

2 Algorithm model

The IVS model is used to implement the automatic inspection method for the LED indicators. The main processes are as follows:

1. Image acquisition: After all the LED indicators on the automobile meter are powered up, RGB color images of all the LED indicators are acquired by the charged-coupled device (CCD) camera, while the positions of the LED indicators are kept constant. Subsequently, the RGB color images are separated into individual R, G, and B intensity images.

2. Region extraction: The SRG algorithm is used to obtain the seeds and extract the regions. Firstly, the

seeds are selected from the gray image. Then, based on the seeds, the corresponding LED indicator regions are extracted in the R, G, and B intensity images. Finally, the area of LED indicator regions is calculated. Seeds and region area parameters from the standard image (where the brightness and color of all the LED indicators are determined to be correct) are treated as the set template.

3. Region matching: Based on seeds and region area parameters, the LED indicator regions in the inspected image are compared one by one with the set template to locate the errors that have occurred in the production process of LED indicators.

The above three steps are described in more detail in the following subsections.

2.1 Image acquisition

In the interior space under common incandescent lamp illumination (about 500 lx), at a distance of about 0.5 m between the visual device and the automobile meter to be inspected, RGB color images of LED indicators are acquired by an industrial CCD camera (MV-300UC). The resolution is 512×384 (24-bit) and the pixel size is 3.2 μm×3.2 μm. An RGB color image is an $M×N×3$ array of color pixels where each color pixel is a triplet corresponding to the red, green, and blue components of an RGB image at a specific spatial location. Therefore, it can be viewed as a stack of three intensity images referred to as the R, G, and B images respectively (Gonzalez *et al.*, 2003). Fig. 2 shows the R, G, and B images separated from an RGB color image of LED indicators.
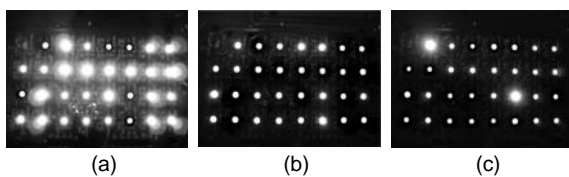
(a)   (b)   (c)

Fig. 2 (a) R, (b) G, and (c) B images taken by an industrial CCD camera (MV-300UC)
The illumination of the environment was about 500 lx. The distance between the camera and the automobile meter to be inspected was about 0.5 m. The resolution was 512×384 (24-bit) and the pixel size was 3.2 μm×3.2 μm

2.2 Region extraction

As it is more complicated to process the color images directly than to process the intensity images, the indicator regions in the R, G, and B intensity images are extracted with the SRG algorithm. In this paper, the SRG algorithm based on Otsu (1979)'s method includes two main processes: a seed auto-selection process and a region growing process.

2.2.1 Seed auto-selection

Fig. 3 shows a gray image of LED indicators, from which the seeds are selected. To achieve the purpose of selecting the seeds automatically, three steps are performed as follows.

Fig. 3 Gray image of LED indicators

Step 1: Otsu's method (Otsu, 1979; Tuduki *et al.*, 2000) is used to determine a threshold and then a binary image is obtained. This method is applied as follows: the histogram of the gray image is divided into two groups, each with a certain intensity distribution. The threshold is defined as the intensity value where the covariance of the two groups reaches the maximum. First, we compute the total number of pixels, N, in the image using

$$N = \sum_{i=0}^{L-1} n_i, \tag{1}$$

where n_i is the number of pixels that have intensity level i, and L is the total number of possible intensity levels in the image. The normalized histogram is given by

$$p_i = n_i / N. \tag{2}$$

Otsu's method chooses threshold k that maximizes the covariance σ^2, which is defined as

$$\sigma^2 = \omega_0 (u_0 - u)^2 + \omega_1 (u_1 - u)^2, \tag{3}$$

where

$$\omega_0 = \sum_{i=0}^{k-1} p_i, \ \ \omega_1 = \sum_{i=k}^{L-1} p_i, \ \ u_0 = \sum_{i-0}^{k-1} ip_i / \omega_0,$$

$$u_1 = \sum_{i=k}^{L-1} ip_i / \omega_1, \ \ u = \sum_{i=0}^{L-1} ip_i.$$

In the gray image shown in Fig. 3, the value of L is 256. The normalized histogram of this image is shown in Fig. 4. With k varying between 0 and 255, the threshold value is selected which maximizes σ^2 as given by Eq. (3); in this case, a k value of 133 is obtained as the optimal threshold value. The binary image can then be generated from the gray image, as in Eq. (4):

$$g'(x, y) = \begin{cases} 255, & g(x, y) \geq k, \\ 0, & \text{otherwise,} \end{cases} \tag{4}$$

where $g(x, y)$ is the value of a pixel from the gray image and $g'(x, y)$ is the value of a pixel from the binary image.
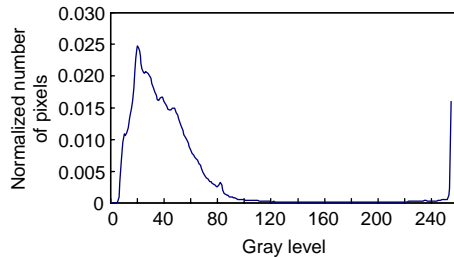

Fig. 4 Normalized histogram of the gray image in Fig. 3

Step 2: If the regions are noisy, single seeds may fall on an atypical pixel and the number of seeds extracted may be more than the true value, which will lead to algorithm errors. Morphology opening (Gonzalez *et al.*, 2003) is applied to eliminate the noise of the binary image. Morphology opening is an erosion followed by a dilation which removes regions of an object that cannot completely contain the structuring element. Fig. 5 shows the result of the binary image generated from the gray image (Fig. 3) after the noise has been eliminated.
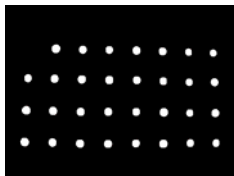

Fig. 5 Binary image after eliminating noise (k=133, a 5×5 square was used as the structuring element)

Step 3: After eliminating the noise of the binary image, the object regions of each LED indicator are segmented. The centroids of these regions are then

extracted as the initial seeds and the coordinates of each seed to the array Se[num, 2] are recorded where num denotes the total number of seed points. In the binary image example shown in Fig. 5, the value of num is 31.

2.2.2 Region growing process

Apart from the seeds, the selection of homogeneous criteria is another key point in the region growing process. In this paper, the gray level difference $\delta(x, y)$ shown in Eq. (5) between the gray value of the pixel and the region mean is applied first as a homogeneous criterion (Adams and Bischof, 1994):

$$\delta(x, y) = \left| g(x, y) - \underset{(x, y) \in S}{\text{mean}}[g(x, y)] \right|, \tag{5}$$

where S is the corresponding region which is being grown and $g(x, y)$ is the gray value of the pixel (x, y) which belongs to the growing region S. Then the region growing processes are performed as follows (Adams and Bischof, 1994; Ikonomatakis *et al.*, 1997).
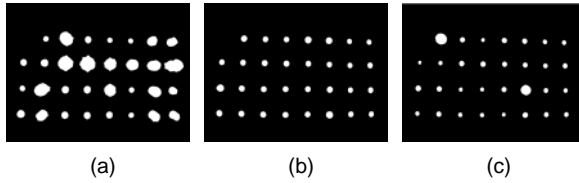
Step 1: A seed is selected from the seed array Se[num, 2] and labeled.

Step 2: The seed is regarded as the center of the region and its 8-neighborhood pixels are tested one by one. If the neighborhood pixel is labeled, then nothing is done. If the neighborhood pixel is not labeled, the gray level difference (Eq. (5)) between the neighborhood pixel and the region mean is calculated; if it is less than a pre-determined threshold T, this pixel is merged and labeled. When all of the neighbors have been tested, the mean of the new region is updated.

Step 3: The pixels, combined with the region in Step 2, are then regarded as the new centers to replace the seed one by one. After selecting one of them as the center, Step 2 is repeated, and all other neighborhood pixels are tested until no new pixels may be merged and the region growing process is completed. Growing a region should stop when no more pixels satisfy the criteria for inclusion in that region.

Step 4: Return to Step 1 until all the seeds have completed the growing process.

The R, G, and B images, shown in Fig. 2, are each segmented using the SRG algorithm according to the above processes. The segmentation results are shown in Fig. 6.
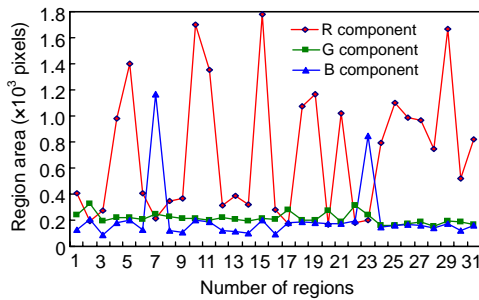
Fig. 6 Results of region growing process (*T*=30)
(a) R component after segmentation; (b) G component after segmentation; (c) B component after segmentation

2.2.3 Characteristic feature extraction

The three area parameters of each region in Fig. 6 are calculated (Fig. 7). The results of region area comparisons are shown in Table 1. Fig. 7 and Table 1 show that different colors have different region area values. For example, red LED indicators have the largest region area in the R component image (>700 pixels), green ones in the G component image (>250 pixels) and blue ones in the B component image (>500 pixels) (Table 1). For the yellow LED indicators, region areas in the R and G images have medium values but in the B image have minimum values. Therefore, the three area parameters corresponding to an LED indicator region can be used to distinguish different colors.

Fig. 7 Three area parameters of each region in R, G, and B component images

Table 1 Comparison of region areas in R, G, and B images[*]

Type of LED indicator	R_area (pixels)	G_area (pixels)	B_area (pixels)
Red	>700	150–250	140–500
Green	<300	>250	140–500
Blue	<300	150–250	>500
Yellow	300–700	150–250	<140

[*] The resolution of the images is 512×384

The three area parameters of each region are saved in the R_area[num], G_area[num], and B_area[num] respectively, according to the sequence of seeds from the array Se[num, 2], where num denotes the total number of regions. The Se[num, 2], R_area[num], G_area[num], and B_area[num] obtained from the standard images are preserved as the set template, denoted as TSe[num, 2], TR_area[num], TG_area[num], and TB_area[num], respectively.

2.3 Region matching

Errors such as malfunctions, low brightness causing poor recognition with the naked eye or incorrect color often occur in LED indicators. To locate these errors, a region matching process is proposed, based on the seeds (Se[num, 2]) and the three area parameters of each region in R, G, and B images (R_area[num], G_area[num], and B_area[num]). Actually, region matching is the same as image comparison where the inspected image is compared with the standard image. In practice, two main situations are considered: first, if the indicator is not functioning properly or the brightness is too low to be recognized with the naked eye, then no seed can be selected in the region of this LED indicator. Second, if the color is wrong, then the three area parameters of this region in the R, G, and B image cannot be matched. The specific process of region matching used is described as follows.

Step 1: The set template, denoted as TSe, TR_area, TG_area, and TB_area, is saved.

Step 2: The seeds of the image under inspection, Se, are compared with the TSe one by one; any LED indicator with a lost seed will be rejected.

Step 3: The three area parameters R_area, G_area, and B_area are compared with TR_area, TG_area, and TB_area respectively, for the images with the correct seeds. The correct color is predetermined by a permissible error ε, as shown in

$$\frac{|\text{X\_area} - \text{TX\_area}|}{\text{TX\_area}} < \varepsilon, \tag{6}$$

where X_area represents R_area, G_area, or B_area, and TX_area represents TR_area, TG_area, or TB_area.

Step 4: The inspection result is returned to the user after the completion of the region matching process.

3 Experimental results

In our experiment, we used an automobile meter with 31 LED indicators including four colors: red, green, blue and yellow (Fig. 2). To evaluate the approach proposed in this paper, 20 of these automobile meters were tested and therefore the total number of the LED indicators was 620 (31×20). These automobile meters were inspected with the automatic inspection method proposed in this paper and the inspection accuracy rate (IAR) was used as the evaluation criterion for the algorithm, as shown in Eq. (7):

$$IAR = \frac{N_R}{N_W + N_R}, \qquad (7)$$

where N_W is the number of false inspection results and N_R is the number of correct inspection results. The results of automatic inspection of the LED indicators are given in Table 2. The results show that the total number of correct inspections was 617 among the 620 LED indicators and the IAR was up to 99.52% (Eq. (7)). A comparison of the IARs and time cost between the manual and the proposed automatic inspection methods is shown in Table 3. To inspect one automobile meter with 31 LED indicators, the manual method cost 60 s on average, but the proposed automatic method cost only 18 s. Thus, the new method greatly improves inspection efficiency.

Table 2 Results of automatic inspection of light emitting diode (LED) indicators (ε=5%)

State of LED indicators	N_R	N_W	N_W+N_R
Working failure	35	0	35
Low brightness[*]	30	0	30
Incorrect color	40	2	42
Functioning normally[**]	512	1	513
Total	617	3	620

N_R: number of correct inspection results; N_W: number of false inspection results. [*] Lack of brightness causing poor recognition with the naked eye within a distance of about 0.5 m. [**] Brightness and color are both determined to be correct

Table 3 Comparison of the inspection accuracy rates (IARs) and time cost between the manual inspection and the automatic inspection

Method	IAR (%)	Time (s)[*]
Manual inspection	95.00	60
Automatic inspection	99.52	18

[*] Time cost in inspecting one automobile meter with 31 LED indicators

4 Discussion

From Table 2, it can be seen that the total number of false inspections was 3, including two kinds of failures: (1) 2 of the 42 LED indicators were diagnosed with incorrect color, and (2) 1 normal functioning LED indicator was diagnosed with incorrect color out of a total of 513. Actually, these two kinds of failures were both related to the color judgment. In our method, the three area parameters of each region in R, G, and B images are used to distinguish color differences. However, from Fig. 7 and Table 1, we can see that even for LED indicators with the same color, their corresponding area parameters can differ greatly. For example, for the red LED indicators in our experiment, the maximal region area of red LED indicators in the R component image was nearly 1800 pixels while the minimum was only about 750 pixels (Fig. 7), which would cause the color misjudgment. Thus, further work is needed to deal with this problem of our approach so as to avoid the color misjudgment and to improve the accuracy rate.

5 Conclusion

This paper presents an automatic inspection method for LED indicators on automobile meters to replace the traditional human visual technique. Two main features of this approach are:

1. To simplify the region extraction process on color images, R, G, and B images are separated from each RGB color image and are then segmented using an SRG algorithm.

2. To inspect the brightness and the color of the LED indicators, seeds and three area parameters of each region in R, G, and B images are taken as the characteristic features to match to a set template.

Experiments have showed that the inspection accuracy rate of this method is up to 99.52% and the inspection time for one automobile meter with 31 LED indicators is 18 s on average. This suggests that there are promising prospects for practical application of the new method.

References

Adamek, T., O'Connor, N., Murphy, N., 2005. Region-Based Segmentation of Images Using Syntactic Visual Features. 6th Int. Workshop Image Analysis for Multimedia Interactive Services, p.1-4.

Adams, R., Bischof, L., 1994. Seeded region growing. *IEEE Trans. Pattern Anal. Mach. Intell.*, **16**(6):641-647. [doi: 10.1109/34.295913]

Buxton, B.F., Abdallahi, H., Delmiro, F.R., Jarra, W., 2007. Development of an Extension of the Otsu Algorithm for Multidimensional Image Segmentation of Thin-Film Blood Slides. Proc. Int. Conf. on Computing: Theory and Applications, p.552-562.

Chang, C.Y., Li, C.H., Lin, S.Y., Jeng, M., 2009. Application of two Hopfield neural networks for automatic four-element LED inspection. *IEEE Trans. Syst. Man Cybern.*, **39**(3):352-365. [doi:10.1109/TSMCC.2009.2013817]

Ghazi Saeidi, R., Latifi, M., Shaikhzadeh Najar, S., Ghazi Saeidi, A., 2005. Computer vision-aided fabric inspection system for on-circular knitting machine. *Textile Res. J.*, **75**(6):492-497. [doi:10.1177/0040517505053874]

Gonzalez, R.C., Woods, R.E., Eddins, S.L., 2003. Digital Image Processing Using MATLAB. Prentice Hall Inc., NJ, USA, p.195-241.

Ikonomatakis, N., Plataniotis, K.N., Zervakis, M., Venetsanopoulos, A.N., 1997. Region Growing and Region Merging Image Segmentation. Proc. 13th Int. Conf. on Digital Signal Processing, p.299-302. [doi:10.1109/ICDSP.1997.628077]

Kumar, A., 2008. Computer-vision-based fabric defect detection: a survey. *IEEE Trans. Ind. Electron.*, **55**(1):348-363. [doi:10.1109/TIE.1930.896476]

Lee, B.Y., Tarng, Y.S., 2001. Surface roughness inspection by computer vision in turning operations. *Int. J. Mach. Tools Manuf.*, **41**(9):1251-1263. [doi:10.1016/S0890-6955(01)00023-2]

Malamas, E.N., Petrakis, E.G.M., Zervakis, M., Petit, L., Legat, J.D., 2003. A survey on industrial vision system, applications and tools. *Image Vis. Comput.*, **21**(2):171-188. [doi:10.1016/S0262-8856(02)00152-X]

Moganti, M., Ercal, F., Dagli, C.H., Tsunekawa, S., 1996. Automatic PCB inspection algorithms: a survey. *Comput. Vis. Image Understand.*, **63**(2):287-313. [doi:10.1006/cviu.1996.0020]

Newman, T.S., Jain, A.K., 1995. A survey of automated visual inspection. *Comput. Vis. Image Understand.*, **61**(2):231-262. [doi:10.1006/cviu.1995.1017]

Otsu, N., 1979. A threshold selection method from gray-level histograms. *IEEE Trans. Syst. Man Cybern.*, **9**(1):62-66. [doi:10.1109/TSMC.1979.4310076]

Pal, N.R., Pal, S.K., 1993. A review on image segmentation techniques. *Pattern Recogn.*, **26**(9):1277-1294. [doi:10.1016/0031-3203(93)90135-J]

Perng, D.B., Chou, C.C., Chen, W.Y., 2007. A novel vision system for CRT panel auto-inspection. *J. Chin. Inst. Ind. Eng.*, **24**(5):341-350.

Tuduki, Y., Murase, K., Izumida, M., Miki, H., Kikuchi, K., Murakami, K., Ikezoe, J., 2000. Automated Seeded Region Growing Algorithm for Extraction of Cerebral Blood Vessels from Magnetic Resonance Angiographic Data. Proc. 22nd Annual Int. Conf. of the IEEE Engineering in Medicine and Biology Society, **3**:1756-1759. [doi:10.1109/IEMBS.2000.900424]

Wu, H.S., Barba, J., Gil, J., 1996. Region growing segmentation of textured cell image. *Electron. Lett.*, **32**(12):1084-1085. [doi:10.1049/el:19960738]

Wu, L.M., Wu, F.J., Wang, G.T., 2008. Computer Vision Inspection for IC Wafer Based on Character of Pixels Distribution. Proc. 3rd Int. Conf. on Convergence and Hybrid Information Technology, **2**:248-251. [doi:10.1109/ICCIT.2008.40]

Zhang, Y.J., 1996. A survey on evaluation methods for image segmentation. *Pattern Recogn.*, **29**(8):1335-1346. [doi:10.1016/0031-3203(95)00169-7]